Shape optimization of a layer-by-layer constraint functional for additive manufacturing processes

Grégoire Allaire[1], Charles Dapogny[2], Rafael Estevez[3], Alexis Faure[3], and Georgios Michailidis[3]

[1] CMAP, UMR 7641 École Polytechnique, Palaiseau, France
[2] CNRS & Laboratoire Jean Kuntzmann, Université Grenoble-Alpes, Grenoble, France
[3] SiMaP, Université Grenoble-Alpes, Grenoble, France

13th October, 2017

Foreword: shape optimization in the industrial context

- Shape and topology optimization techniques have aroused a tremendous enthusiasm within the engineering and industrial communities.
- One drawback of these methods is that the optimized designs are often too complicated to be constructed by traditional methods such as milling or casting.
- The recent headway made by additive manufacturing methods allow to assemble structures with a high degree of complexity.
- These techniques impose new constraints on the manufactured components.

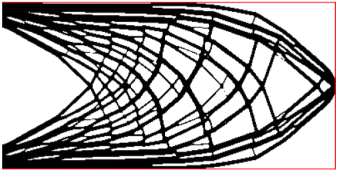

Typical 'truss' designs resulting from shape and topology optimization processes.

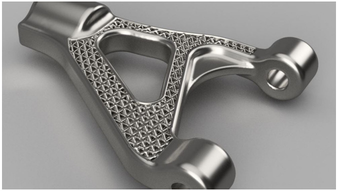

Part produced with an additive manufacturing method (from `http://www.autodesk.com/`*).*

Additive manufacturing in a nutshell

- All the additive manufacturing processes begin with a slicing stage: the input shape is decomposed into a series of horizontal layers.
- These $2d$ layers are built one on top of the other according to the selected technology, e.g. material extrusion, or powder bed fusion methods.

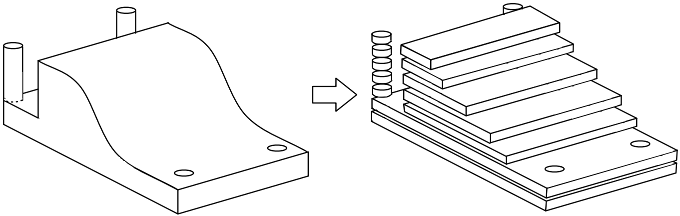

Sketch of the slicing procedure, initiating any additive manufacturing process.

The overhang issue (I)

All additive manufacturing technologies experience trouble in the assembly of shapes showing large overhangs, i.e. regions hanging over void.

- in the case of material extrusion methods, this amounts to assembling over void.
- In the case of powder-bed methods, the rapid melting then solidification of the powder induces residual stress, especially in regions unanchored to the lower structure. This may cause warpage of such parts upon cooling.

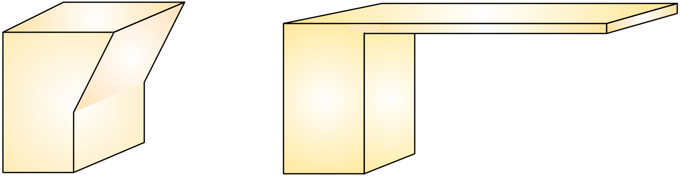

(Left) short overhang; support from the lower structure is sufficient to guarantee manufacturability; (right) large overhang.

The overhang issue (II)

- The most common strategy to deal with overhangs is to erect a sacrificial scaffold structure alongside the construction of the shape [DuHeLe].
- This scaffold has to be removed as a (costly and cumbersome) post-processing $\Rightarrow$ Need to impose that the structure be self-supporting since the design stage.

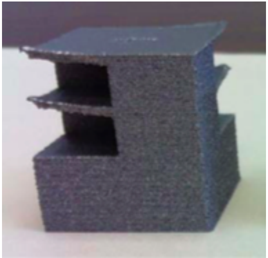

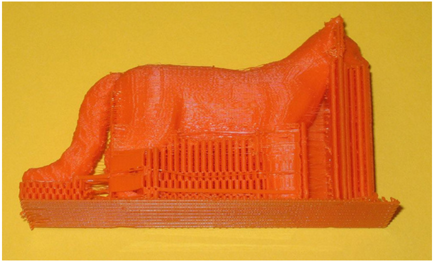

(Left) Warpage caused by residual constraints in an EBM assembly (from [CheLuChou]), (right) scaffold structure in the construction of a part (from `https://hyrulefoundry.wordpress.com/`).

- Literature about overhang constraints include: [BraAshHa], [GayGue], [Lan], [LeaMeToMaBra], [MaAm], [MirSur], [Qia].

Shape optimization of linear elastic shapes (I)

In the context of its final use, a shape is a bounded domain $\Omega \subset \mathbb{R}^d$, which is

- fixed on a part Γ_D of its boundary,
- submitted to surface loads f, applied on $\Gamma_N \subset \partial\Omega$, $\Gamma_D \cap \Gamma_N = \emptyset$.

The displacement vector field $u_\Omega : \Omega \to \mathbb{R}^d$ is governed by the linear elasticity system:

$$\begin{cases} -\text{div}(Ae(u_\Omega)) & = & 0 & \text{in } \Omega \\ u_\Omega & = & 0 & \text{on } \Gamma_D \\ Ae(u_\Omega)n & = & f & \text{on } \Gamma_N \\ Ae(u_\Omega)n & = & 0 & \text{on } \Gamma \end{cases},$$

where $e(u) = \frac{1}{2}(\nabla u^T + \nabla u)$ is the strain tensor, and A is the Hooke's law of the material:

$$\forall e \in \mathcal{S}_d(\mathbb{R}), \;\; Ae = 2\mu e + \lambda \text{tr}(e) I.$$

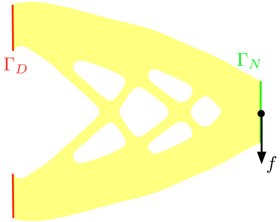

A 'Cantilever'

The deformed cantilever

The shape optimization problem

The shape optimization problem of interest reads:

$$\min_{\mathcal{U}_{\mathrm{ad}}} J(\Omega), \text{ s.t. } P(\Omega) \leq \alpha,$$

in which

- $\mathcal{U}_{\mathrm{ad}}$ is a set of (smooth) admissible shapes,
- The objective function $J(\Omega)$ is the structural compliance of shapes:

$$J(\Omega) = \int_{\Omega} Ae(u_\Omega) : e(u_\Omega)\, dx = \int_{\Gamma_N} f \cdot u_\Omega \, ds,$$

- The constraint $P(\Omega)$ enforces the constructibility by additive manufacturing processes,
- Other constraints may be added to the problem, e.g. on the volume $\mathrm{Vol}(\Omega)$ of shapes.

Differentiation with respect to the domain: Hadamard's method

Hadamard's boundary variation method describes variations of a reference domain Ω of the form:

$$\Omega \to \Omega_\theta := (\mathrm{Id} + \theta)(\Omega),$$

for 'small' vector fields $\theta : \mathbb{R}^d \to \mathbb{R}^d$.

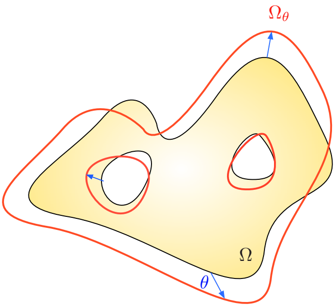

Definition 1.

Given a smooth domain Ω, a function $J(\Omega)$ of the domain is shape differentiable at Ω if the function

$$\theta \mapsto J(\Omega_\theta)$$

is differentiable at 0, i.e. the following expansion holds around 0:

$$J(\Omega_\theta) = J(\Omega) + J'(\Omega)(\theta) + o\left(||\theta||\right).$$

Techniques from optimal control theory make it possible to calculate shape derivatives; in the case of 'many' functionals of the domain $J(\Omega)$, the shape derivative has the particular structure:

$$J'(\Omega)(\theta) = \int_\Gamma v_\Omega \, \theta \cdot n \, ds,$$

where v_Ω is a scalar field depending on u_Ω, and possibly on an adjoint state p_Ω.

Example: If the objective function

$$J(\Omega) = \int_{\Gamma_N} f \cdot u_\Omega \, ds$$

is the compliance, $v_\Omega = -Ae(u_\Omega) : e(u_\Omega)$ is the (negative) elastic energy density.

The generic algorithm

This shape gradient provides a natural descent direction for $J(\Omega)$: *for instance*, defining θ as

$$\theta = -v_\Omega n$$

yields, for $t > 0$ sufficiently small (*to be found numerically*):

$$J((\mathrm{Id} + t\theta)(\Omega)) = J(\Omega) - t\int_\Gamma v_\Omega^2 ds + o(t) < J(\Omega)$$

Gradient algorithm: For $n = 0, \ldots$ until convergence,

1. Compute the solution u_{Ω^n} (and p_{Ω^n}) of the elasticity system on Ω^n.
2. Compute the shape gradient $J'(\Omega^n)$ thanks to the previous formula, and infer a descent direction θ^n for the cost functional.
3. Advect the shape Ω^n according to θ^n, so as to get $\Omega^{n+1} := (\mathrm{Id} + \theta^n)(\Omega^n)$.

The 'naive', geometric attempt (I)

- Most approaches in the literature rely on the angle between $\partial\Omega$ and the (vertical) build direction to detect and penalize overhangs.
- An intuitive approach relies on anisotropic perimeter functionals of the form:

$$P_g(\Omega) = \int_{\partial\Omega} \varphi(n_\Omega)\, ds, \text{ where } \varphi : \mathbb{R}^d \to \mathbb{R} \text{ is given.}$$

Example The choice $\varphi_a(n) := (n \cdot e_d + \cos\nu)_-^2$, where $(s)_- := \min(s, 0)$, penalizes regions of $\partial\Omega$ where the angle $n \cdot (-e_d)$ is smaller than a threshold ν.

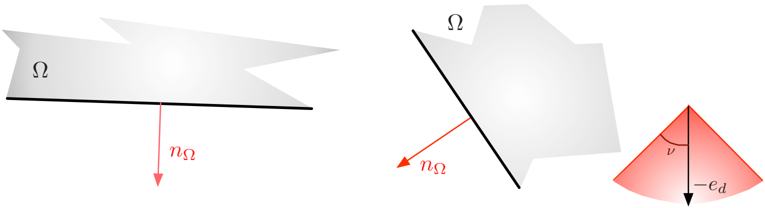

Parts of $\partial\Omega$ (left) violating and (right) satisfying the angle-based criterion.

The 'naive', geometric attempt (II)

Proposition 1.

The functional $P_g(\Omega)$ is shape differentiable at any admissible shape $\Omega \in \mathcal{U}_{\text{ad}}$, and its shape derivative reads:

$$P_g'(\Omega)(\theta) = \int_\Gamma \kappa\, \varphi(n)\, \theta \cdot n \, ds - \int_\Gamma \nabla(\varphi(n)) \cdot \nabla_{\partial\Omega}(\theta \cdot n)\, ds,$$

where $\nabla_{\partial\Omega}\psi := \nabla\psi - (\nabla\psi \cdot n)n$ is the tangential gradient of a function $\psi : \partial\Omega \to \mathbb{R}$, and κ is the mean curvature of $\partial\Omega$.

- Unfortunately, this approach gives unsatisfactory results in our context.
- We will propose instead a general idea for modeling overhang constraints, which appeals to their mechanical origin.

Geometric constraints; the 'dripping effect' (I)

We consider the two-dimensional MBB Beam example.

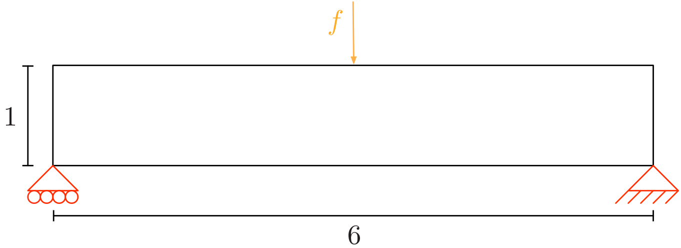

Setting of the two-dimensional MBB beam example.

We first solve the compliance minimization problem:

$$\begin{array}{ll} \min_{\Omega} & J(\Omega), \\ \text{s.t.} & \text{Vol}(\Omega) \leq \alpha_v \text{Vol}(D). \end{array}$$

Geometric constraints; the ‘dripping effect’ (II)

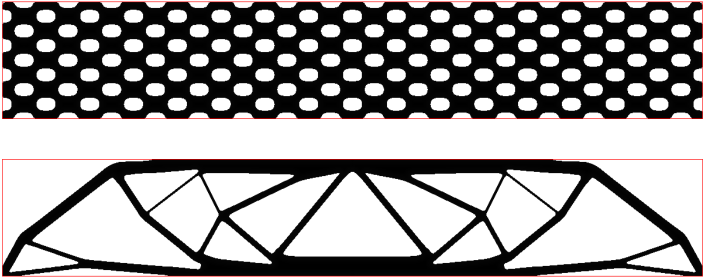

(Top) initial shape Ω_0 and (bottom) optimized shape Ω^* for compliance minimization in the two-dimensional MBB Beam example.

The optimized shape Ω^* presents large nearly horizontal bars which are very important for the structural performance.

Geometric constraints; the 'dripping effect' (III)

To help in removing these overhangs, we rather solve the problem:

$$\begin{aligned} \min_{\Omega} \quad & (1-\alpha_g)\frac{J(\Omega)}{J(\Omega^*)} + \alpha_g \frac{P_g(\Omega)}{P_g(\Omega^*)}, \\ \text{s.t.} \quad & \text{Vol}(\Omega) \leq \alpha_v \text{Vol}(D). \end{aligned}$$

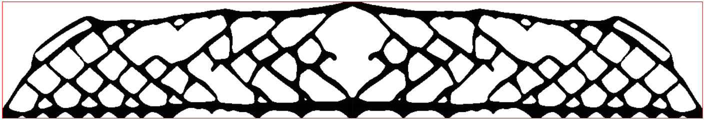

Optimized shape using $\alpha_g = 0.5$.

The shape develops an oscillatory boundary so that:

- The angle requirement is (approximately) satisfied,
- The structural performance is not too much altered: the large bars connecting loads to anchor points have not disappeared.

Definition of the mechanical constraint (I)

The mechanical constraint $P(\Omega)$ relies on the physical behavior of the shape at each stage of its construction.

- Ω is enclosed in the build chamber $D = S \times (0, H)$, where $S \subset \mathbb{R}^{d-1}$,
- $\Omega_h := \{x = (x_1, ..., x_d) \in \Omega, \ x_d < h\}$ is the intermediate shape at height h.
- The boundary $\partial\Omega_h$ is decomposed as $\partial\Omega_h = \Gamma_0 \cup \Gamma_h^u \cup \Gamma_h^l$, where
  - $\Gamma_0 = \{x \in \partial\Omega_h, \ \ x_d = 0\}$ is the contact region between Ω and the build table,
  - $\Gamma_h^u = \{x \in \partial\Omega_h, \ \ x_d = h\}$ is the upper side of Ω_h,
  - $\Gamma_h^l = \partial\Omega_h \setminus (\overline{\Gamma_0} \cup \overline{\Gamma_h^u})$ is the lateral surface.

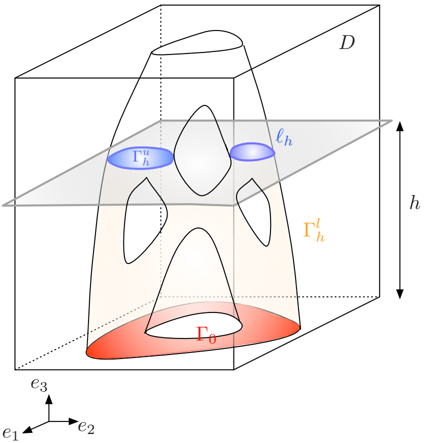

Definition of the mechanical constraint (II)

- Each intermediate shape Ω_h is only subjected to gravity effects $g : \mathbb{R}^d \to \mathbb{R}^d$. The elastic displacement of Ω_h satisfies:

$$\begin{cases} -\mathrm{div}(Ae(u_{\Omega_h^c})) = g & \text{in } \Omega_h, \\ u^c_{\Omega_h} = 0 & \text{on } \Gamma_0, \\ Ae(u^c_{\Omega_h})n = 0 & \text{on } \Gamma_h^l \cup \Gamma_h^u. \end{cases}$$

- The self-weight of each intermediate shape Ω_h is:

$$c_{\Omega_h} := \int_{\Omega_h} Ae(u^c_{\Omega_h}) : e(u^c_{\Omega_h})\, dx = \int_{\Omega_h} g \cdot u^c_{\Omega_h}\, dx.$$

- The (self-weight) manufacturing compliance of a final shape Ω aggregates the self-weights of all its intermediate shapes:

$$P_{\mathrm{sw}}(\Omega) = \int_0^H j(c_{\Omega_h})\, dh,$$

where $j : \mathbb{R} \to \mathbb{R}$ is a given function.

Shape derivative of the manufacturing compliance

- We consider a fixed shape $\Omega \in \mathcal{U}_{\mathrm{ad}}$.
- Perturbations θ are confined to a class X^k of vector fields of class $\mathcal{C}^k$, which identically vanish near the 'flat regions' of $\partial\Omega$.

Theorem 2.

The manufacturing compliance $P_{\mathrm{sw}}(\Omega)$ is shape differentiable at Ω: the mapping $\theta \mapsto P_{\mathrm{sw}}(\Omega_\theta)$, from X^k into $\mathbb{R}$ is differentiable for $k \geq 1$, and its derivative is:

$$\forall \theta \in X^k, \;\; P'_{\mathrm{sw}}(\Omega)(\theta) = \int_{\partial\Omega \setminus \overline{\Gamma_0}} \mathcal{D}_\Omega \, \theta \cdot n \, ds,$$

where the integrand factor $\mathcal{D}_\Omega$ is defined by:

$$\mathcal{D}_\Omega(x) = \int_{x_d}^{H} j'(c_{\Omega_h}) \left(2g \cdot u^c_{\Omega_h} - Ae(u^c_{\Omega_h}) : e(u^c_{\Omega_h}) \right)(x) \, dh.$$

Other models

Other models may be used for the physical behavior of intermediate shapes Ω_h. For instance,

- The definition of $u^c_{\Omega_h}$ could be replaced by:

$$\left\{ \begin{array}{cl} -\text{div}(Ae(u^a_{\Omega_h})) = g_h & \text{in } \Omega_h, \\ u^a_{\Omega_h} = 0 & \text{on } \Gamma_0, \\ Ae(u^a_{\Omega_h})n = 0 & \text{on } \Gamma^l_h, \\ Ae(u^a_{\Omega_h})n = 0 & \text{on } \Gamma^u_h, \end{array} \right. \quad \text{where } g_h(x) = \left\{ \begin{array}{ll} g & \text{if } x_d \in (h-\delta, h), \\ 0 & \text{otherwise,} \end{array} \right.$$

  is an artificial force acting on the upper side of Ω_h. As we shall see, this formulation is better at penalizing perfectly horizontal parts hanging over void.

- The mechanical constraint $P(\Omega)$ could involve the solutions v_{Ω_h} to a thermal cooling problem posed on Ω_h, to model e.g. residual stresses in the final shape Ω; see [AlJak].

Numerical evaluation of $P_{\mathrm{sw}}(\Omega)$ and $P'_{\mathrm{sw}}(\Omega)(\theta)$

- The expressions for $P_{\mathrm{sw}}(\Omega)$ and its derivative $P'_{\mathrm{sw}}(\Omega)(\theta)$

$$P_{\mathrm{sw}}(\Omega) = \int_0^H j(c_{\Omega_h})\, dh, \text{ and } P'_{\mathrm{sw}}(\Omega)(\theta) = \int_{\partial\Omega\setminus\overline{\Gamma_0}} \mathcal{D}_\Omega\, \theta \cdot n \, ds,$$

  where

$$\mathcal{D}_\Omega(x) = \int_{x_d}^H j'(c_{\Omega_h}) \left(2g \cdot u^c_{\Omega_h} - Ae(u^c_{\Omega_h}) : e(u^c_{\Omega_h})\right)(x)\, dh.$$

  involve a continuum of shapes Ω_h via the self-weights c_{Ω_h} and the elastic displacements $u^c_{\Omega_h}$,

- Hence the need for a suitable discretization of $h \mapsto c_{\Omega_h}$ and $h \mapsto u^c_{\Omega_h}$.
- We present:
  - 0^{th}-order approximations P^0_N and $\mathcal{D}^0_N$ of $P_{\mathrm{sw}}(\Omega)$ and $\mathcal{D}_\Omega$,
  - First-order approximations P^1_N and $\mathcal{D}^1_N$ based on an interpolation procedure.

The 'naive', 0^{th} order method

- The height interval $(0, H)$ is discretized with a sequence:

$$0 < h_1 < h_2 < \ldots < h_N = H.$$

- On each interval $I_i := (h_i, h_{i+1})$, we approximate $h \mapsto c_{\Omega_h}$ and $h \mapsto u^c_{\Omega_h}$ by constant quantities:

$$c_{\Omega_h} \approx c_{\Omega_{h_{i+1}}}, \text{ and } u^c_{\Omega_h} \approx u^c_{\Omega_{h_{i+1}}} \text{ on } \Omega_h, \text{ for } h \in (h_i, h_{i+1}).$$

- These approximations are used in the formulas for $P_{\text{sw}}(\Omega)$ and $P'_{\text{sw}}(\Omega)(\theta)$ to obtain the reconstructions P^0_N and $\mathcal{D}^0_N$.

- This method is costly in practice, since it requires a fine discretization $\{h_i\}$ of $(0, H)$ to be accurate enough.

A first-order interpolation method (I)

- On each interval I_i, we approximate $h \mapsto c_{\Omega_h}$ by a cubic spline $h \mapsto \widetilde{c}_i(h)$ by using the data:

$$\widetilde{c}_i(h_i) = c_{\Omega_{h_i}}, \;\; \widetilde{c}_i(h_{i+1}) = c_{\Omega_{h_{i+1}}}, \;\; \widetilde{c}_i{}'(h_i) = \frac{d}{dh}(c_{\Omega_h})\Big|_{h_i},$$

$$\text{and } \widetilde{c}_i{}'(h_{i+1}) = \frac{d}{dh}(c_{\Omega_h})\Big|_{h_{i+1}}.$$

- On each interval I_i, we approximate $h \mapsto u^c_{\Omega_h}$ by:

$$u^c_{\Omega_h}(x) \approx u^c_{\Omega_{h_{i+1}}}(x) + (h_{i+1} - h)\, U_{\Omega_{h_{i+1}}}(x), \text{ a.e. } x \in \Omega_h,$$

where U_{Ω_h} is the 'derivative' of the mapping $h \mapsto u^c_{\Omega_h}$... in a suitable sense ($\approx$ shape derivative).

- These quantities are used in the definitions of $P_{\rm sw}(\Omega)$ and $P'_{\rm sw}(\Omega)(\theta)$ to obtain the approximations P^1_N and $\mathcal{D}^1_N$.

Mechanical approach: the manufacturing compliance (I)

Still in the setting of the two-dimensional MBB Beam example,

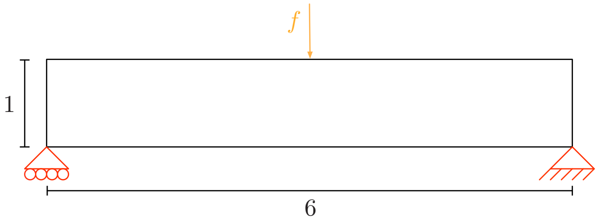

we now solve the constrained optimization problem:

$$\begin{aligned} \min_{\Omega} \quad & J(\Omega) \\ \text{s.t.} \quad & \mathrm{Vol}(\Omega) \leq \alpha_v \mathrm{Vol}(D), \\ & P_{\mathrm{sw}}(\Omega) \leq \alpha_c P_{\mathrm{sw}}(\Omega^*), \end{aligned}$$

where $\alpha_c \in [0, 1]$ is a user-defined tolerance, and Ω^* is the optimized shape for the compliance under volume constraint (without additive manufacturing constraint).

Mechanical approach: the manufacturing compliance (II)

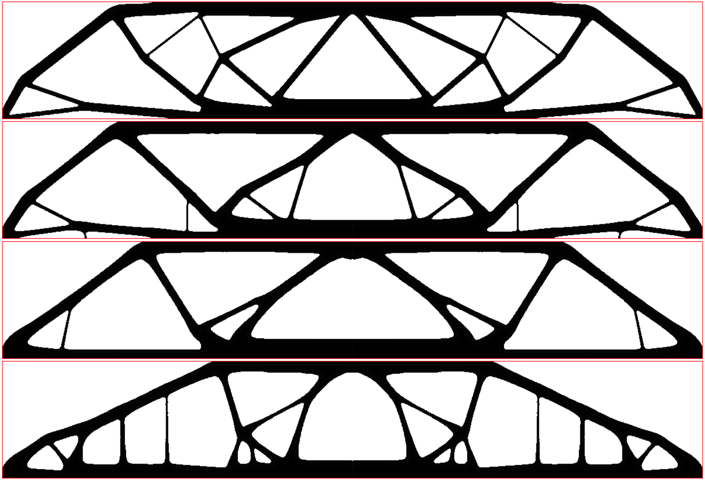

Optimized shapes for the two-dimensional MBB Beam example; (top) optimized shape Ω^*, without additive manufacturing constraints, and optimized shapes using parameters (from top to bottom) $\alpha_c = 0.50$, $\alpha_c = 0.30$, *and* $\alpha_c = 0.10$.

Mechanical approach: the manufacturing compliance (III)

This new approach yields better results; yet, it raises two issues:

1. $P_{\mathrm{sw}}(\Omega)$ inherently favors structures whose lower part is stronger.
2. The optimized shapes still show large, completely horizontal overhangs. This is a flaw in the modelling of $P_{\mathrm{sw}}(\Omega)$, which assumes that each layer of material is assembled instantaneously.

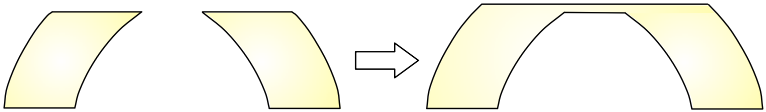

Completely flat overhangs are not so weak because of the instantaneous layer deposition assumption.

Mechanical approach: the modified manufacturing compliance (I)

We now solve:

$$\begin{array}{ll} \min\limits_{\Omega} & J(\Omega) \\ \text{s.t.} & \text{Vol}(\Omega) \leq \alpha_v \text{Vol}(D), \\ & P_{\text{uw}}(\Omega) \leq \alpha_c P_{\text{uw}}(\Omega^*), \end{array}$$

where the modified (upper weight) manufacturing compliance $P_{\text{uw}}(\Omega)$ brings into play elastic displacements of the intermediate shapes $u^a_{\Omega_h}$ involving an artificial load concentrated on their upper side:

$$\left\{ \begin{array}{ll} -\text{div}(Ae(u^a_{\Omega_h})) = g_h & \text{in } \Omega_h, \\ u^a_{\Omega_h} = 0 & \text{on } \Gamma_0, \\ Ae(u^a_{\Omega_h})n = 0 & \text{on } \Gamma^l_h, \\ Ae(u^a_{\Omega_h})n = 0 & \text{on } \Gamma^u_h, \end{array} \right. \quad \text{where } g_h(x) = \left\{ \begin{array}{ll} g & \text{if } x_d \in (h-\delta, h), \\ 0 & \text{otherwise.} \end{array} \right.$$

Mechanical approach: the modified manufacturing compliance (II)

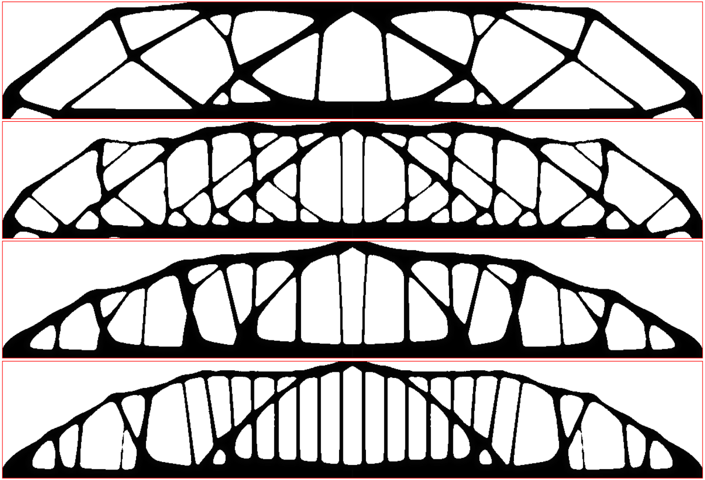

Optimized 2d MBB Beams obtained using the modified manufacturing compliance $P_{\rm af}(\Omega)$ *and parameters (from top to bottom)* $\alpha_c = 0.30$, $\alpha_c = 0.10$, $\alpha_c = 0.05$, *and* $\alpha_c = 0.03$.

We now consider the design of a three-dimensional bridge.

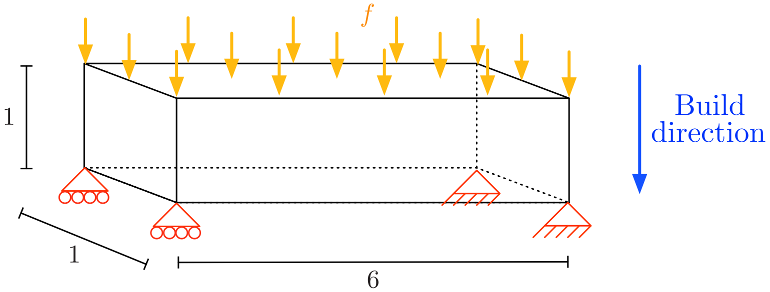

We solve the following shape optimization problem:

$$\begin{array}{ll} \min\limits_{\Omega} & \mathrm{Vol}(\Omega), \\ \text{s.t.} & J(\Omega) \leq J(\Omega^*), \\ & P_{\mathrm{uw}}(\Omega) \leq \alpha_c P_{\mathrm{uw}}(\Omega^*). \end{array}$$

Mechanical approach: the modified manufacturing compliance (IV)

The optimized shape Ω^* without manufacturing shows several large overhangs.

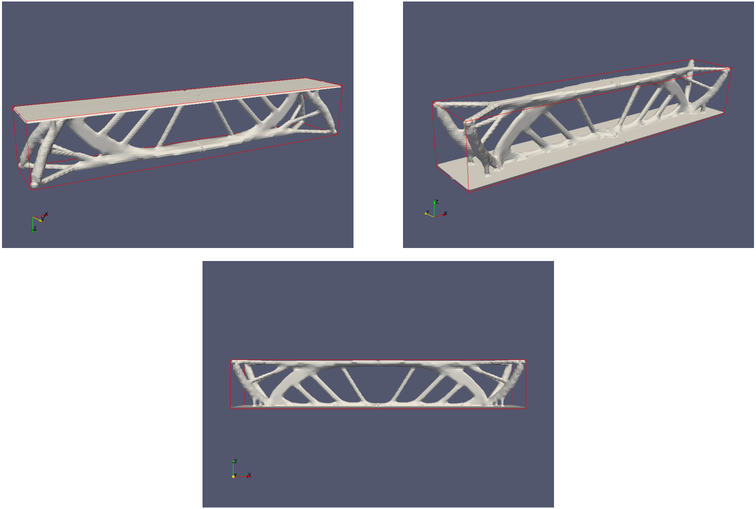

Different views of the unconstrained optimized shape Ω^*.

Mechanical approach: the modified manufacturing compliance (V)

These large overhangs are removed by imposing the manufacturing constraint $P_{\mathrm{uw}}(\Omega)$.

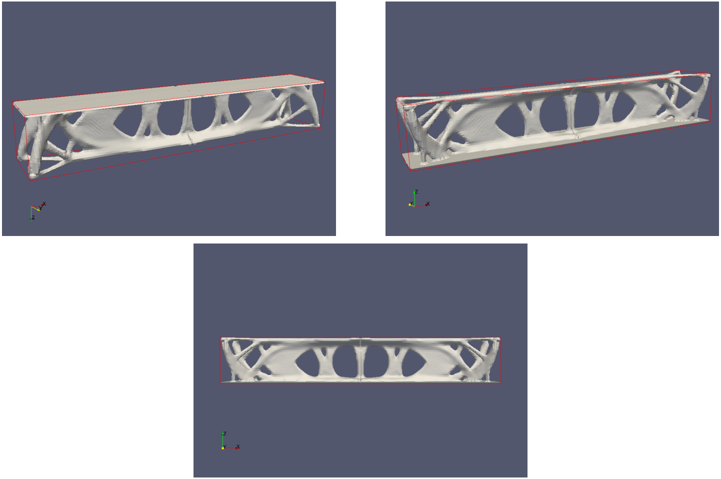

Different views of the optimized shape for $\alpha_c = 0.1$.

Thank you for your attention!

References I

[AlJak] G. Allaire, L. Jakabcin, *Taking into account thermal residual stresses in topology optimization of structures built by additive manufacturing*, (in preparation).

[AlDaFauMiEs] G. Allaire, C. Dapogny, A. Faure, G. Michailidis and R. Estevez, *Shape optimization of a layer by layer mechanical constraint for additive manufacturing*, accepted for publication in C. R. Math. Acad. Sci. Paris. HAL preprint: hal-01398877 (2016).

[AlDaFauMiEs2] G. Allaire, C. Dapogny, A. Faure, G. Michailidis and R. Estevez, *Structural optimization under overhang constraints imposed by additive manufacturing technologies*, to appear in J. Comput. Phys., (2017).

[BraAshHa] D. Brackett, I. Ashcroft, and R. Hague, *Topology optimization for additive manufacturing*, in Proceedings of the Solid Freeform Fabrication Symposium, Austin, TX, 2011, pp. 348–362.

[CheLuChou] B. Cheng, P. Lu and K. Chou, *Thermomechanical Investigation of Overhang Fabrications In Electron Beam Additive Manufacturing*, ASME 2014 International Manufacturing Science and Engineering Conference, (2014).

References II

[DuHeLe] J. Dumas, J. Hergel and S. Lefebvre, *Bridging the Gap: Automated Steady Scaffoldings for 3D Printing*, ACM Trans. Graph., 33, 4, (2014), pp. 1–10.

[GayGue] A. T. Gaynor and J. K. Guest, *Topology optimization considering overhang constraints: Eliminating sacrificial support material in additive manufacturing through design*, Structural and Multidisciplinary Optimization, 54 (2016), pp. 1157–1172.

[GiRoStu] I. Gibson, D.W. Rosen and B. Stucker, *Additive manufacturing technology: rapid prototyping to direct digital manufacturing*, Springer Science Business Media, Inc, (2010).

[Lan] M. Langelaar, *An additive manufacturing filter for topology optimization of print-ready designs*, Structural and Multidisciplinary Optimization, (2016), pp. 1–13.

References III

[LeaMeToMaBra] M. Leary, L. Merli, F. Torti, M. Mazur, and M. Brandt, *Optimal topology for additive manufacture: a method for enabling additive manufacture of support-free optimal structures*, Materials & Design, 63 (2014), pp. 678–690.

[MaAm] Y. Mass and O. Amir, *Topology optimization for additive manufacturing: Accounting for overhang limitations using a virtual skeleton*, Additive Manufacturing,18, (2017), pp. 58-73.

[MirSur] A. M. Mirzendehdel and K. Suresh, *Support structure constrained topology optimization for additive manufacturing*, Computer-Aided Design, 81 (2016), pp. 1–13.

[Qia] X. Qian, *Undercut and overhang angle control in topology optimization: a density gradient based integral approach*, International Journal for Numerical Methods in Engineering, (2017), pp. 247–272.

Mechanical approach, manufacturing compliance (I)

We evaluate the error entailed by the first-order algorithm in terms of the quantities:

$$\mathrm{err}(P, N, i) = \frac{|P_N^i - P_{100}^0|}{P_{100}^0} \quad \text{and} \quad \mathrm{err}(\mathcal{D}, N, i) = \frac{||\mathcal{D}_N^i - \mathcal{D}_{100}^0||_{L^2(\partial\Omega\setminus\overline{\Gamma_0})}}{||\mathcal{D}_{100}^0||_{L^2(\partial\Omega\setminus\overline{\Gamma_0})}}.$$

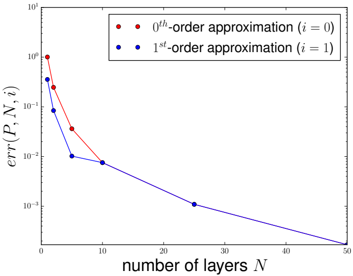

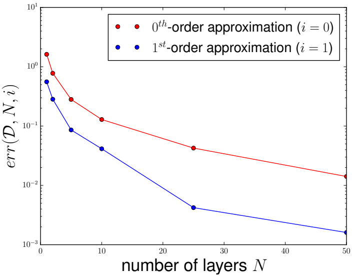

Relative errors of the $0^{\rm th}$*- and* $1^{\rm st}$*-order approximations of* $P_{\rm sw}(\Omega)$ *and its derivative* $\mathcal{D}_\Omega$*.*

The Level Set Method

A paradigm: [?] *the motion of an evolving domain is best described in an implicit way.*

A domain $\Omega \subset \mathbb{R}^d$ is equivalently defined by a function $\phi : \mathbb{R}^d \to \mathbb{R}$ such that:

$$\phi(x) < 0 \quad \text{if } x \in \Omega \quad ; \quad \phi(x) = 0 \quad \text{if } x \in \partial\Omega \quad ; \quad \phi(x) > 0 \quad \text{if } x \in {}^c\overline{\Omega}$$

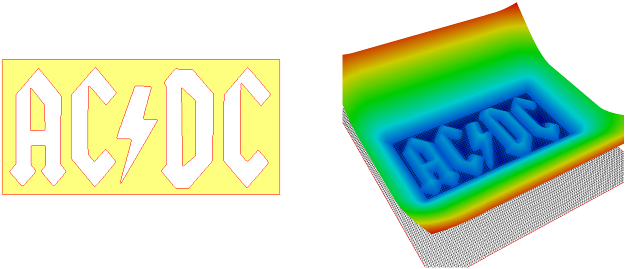

A domain $\Omega \subset \mathbb{R}^2$ (left); graph of an associated level set function (right).

The Level Set Method

The motion of an evolving domain $\Omega(t) \subset \mathbb{R}^d$ along a velocity field $v(t,x) \in \mathbb{R}^d$ translates in terms of an associated 'level set function' $\phi(t,.)$ into the Level Set advection equation:

$$\forall t,\ \forall x \in \mathbb{R}^d,\ \frac{\partial \phi}{\partial t}(t,x) + v(t,x).\nabla\phi(t,x) = 0$$

In many applications, the velocity $v(t,x)$ is normal to the boundary $\partial\Omega(t)$:

$$v(t,x) := V(t,x)\frac{\nabla\phi(t,x)}{|\nabla\phi(t,x)|}.$$

Then the evolution equation rewrites as a Hamilton-Jacobi equation:

$$\forall t,\ \forall x \in \mathbb{R}^d,\ \frac{\partial \phi}{\partial t}(t,x) + V(t,x)|\nabla\phi(t,x)| = 0$$

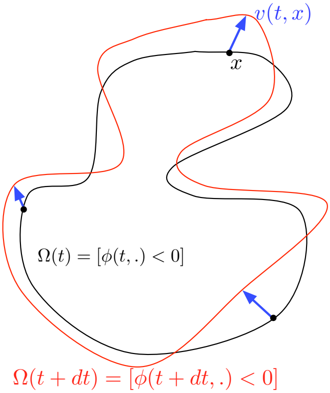

The level set method for shape optimization [?]

- The shapes Ω^n are embedded in a working domain D equipped with a fixed mesh.
- The successive shapes Ω^n are accounted for in the level set framework, i.e. via a function $\phi^n : D \to \mathbb{R}$ which implicitly defines them.
- The linear elasticity equations cannot be solved on Ω^n.

  $\Rightarrow$ Ersatz material approximation: the holes $D \setminus \overline{\Omega^n}$ are filled with a 'very soft material' with Hooke's law εA, $\varepsilon \ll 1$.
- This approach is very versatile and does not require a mesh of the shapes at each iteration.

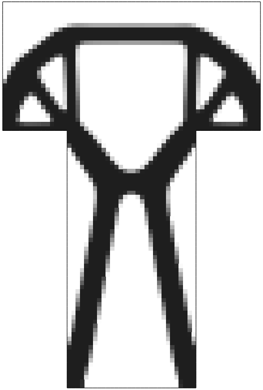

Shape accounted for with a level set description

Geometric constraints; the 'dripping effect' (IV)

Adding a perimeter constraint to the problem is a tentative remedy, but does not prove sufficient to deal with this issue.

Optimized shape using angle and perimeter penalization.

A first-order interpolation method (II)

The derivative of $h \mapsto u^c_{\Omega_h}$ may be thought of as the shape (or Eulerian) derivative of the mapping $t \mapsto u^c_{T_t(\Omega_h)}$, where $T_t : \Omega_h \to \Omega_{h-t}$ is 'any' diffeomorphism from Ω_h onto Ω_{h-t}.

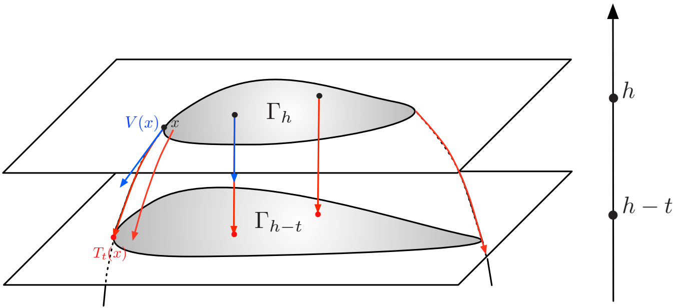

One diffeomorphism T_t mapping Ω_h onto Ω_{h-t}.

Mixing geometric and mechanical formulations (I)

To remedy these completely flat regions caused by the instantaneous layer deposition, we consider the following optimization problem, which mixes geometric and mechanical constraints:

$$\begin{aligned} \min_{\Omega} \quad & (1-\alpha_g)\frac{\mathrm{Vol}(\Omega)}{\mathrm{Vol}(\Omega^*)} + \alpha_g \frac{P_g(\Omega)}{P_g(\Omega^*)}, \\ \text{s.t.} \quad & J(\Omega) \le J(\Omega^*). \\ & P_{\mathrm{uw}}(\Omega) \le \alpha_c P_{\mathrm{uw}}(\Omega^*). \end{aligned}$$

Mixing geometric and mechanical formulations (II)

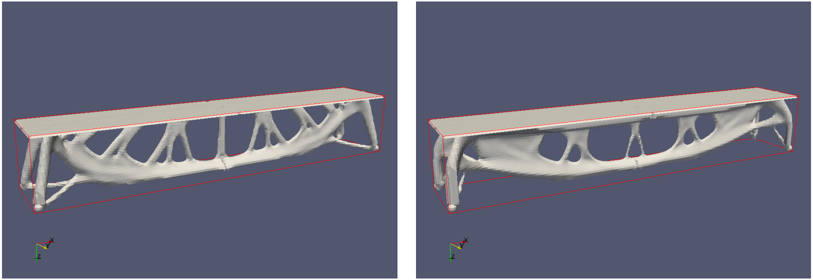

Optimized 3d bridges for the combined geometrically and mechanically constrained problem, setting (left) $\alpha_c = 0.10$, $\alpha_g = 0.10$, *and (right)* $\alpha_c = 0.10$, $\alpha_g = 0.90$.

Mixing geometric and mechanical formulations (III)

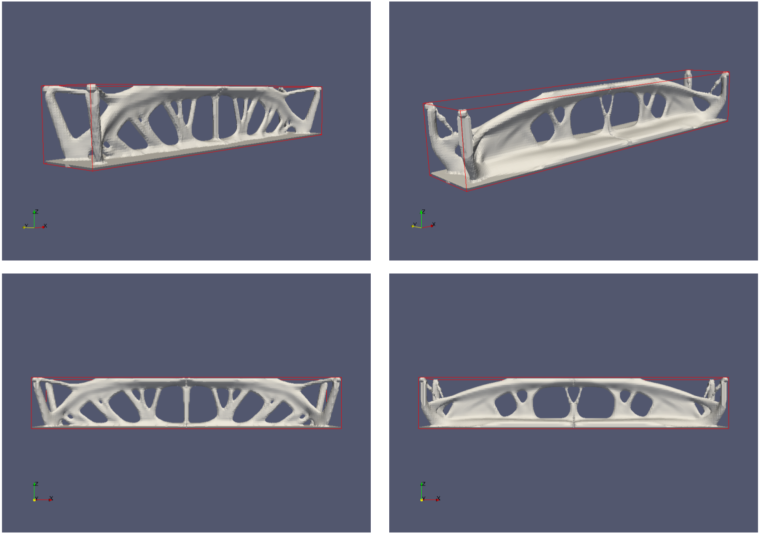

Different views of the optimized shapes with (left) $\alpha_c = 0.10$, $\alpha_g = 0.10$, *and (right)* $\alpha_c = 0.10$, $\alpha_g = 0.90$.